Daytime Sky Brightness Modeling of Haleakala along the GEO Belt

Kevin T.C. Jim, Brooke N. Gibson, Edward A. Pier
Oceanit, Oceanit Center, 828 Fort St. Mall, Suite 600, Honolulu, HI 96813

ABSTRACT

We model the brightness of the daytime sky along the GEO belt, as seen from Haleakala, from 0.3 to 5 μm using MODTRAN. A model near summer solstice and near vernal equinox will illustrate how the sky brightness changes with season. Our goal is to determine the sky background radiance and transmission as a function of wavelength for imaging applications during the daytime. The sky brightness varies throughout a modeled day, and this is shown using a set of look angles toward the geosynchronous belt. We compare our results using radiosonde and real weather data recorded at the summit on two dates, one near the vernal equinox and one near the summer solstice.

1. INTRODUCTION

Optical telescope systems used during the day for satellite tracking could prove to be a useful addition to the SSN. While the SSN currently uses radar for daytime GEO satellite tracking, the operation and maintenance is expensive and their coverage is limited. Daytime optical systems could be deployed in areas lacking coverage by radars and could reduce expenses while also providing additional satellite characterization capabilities such as photometry.

The bright daytime sky poses the main challenge of operating and developing a daytime optical system. Modeling the sky radiance and transmittance at potential sites assists in finding system requirements such as optimal filter bandpass and in predicting the performance of such an optical system. When empirical weather and radiosonde data from specific sites are used, the models can be more accurate [1]. This type of modeling can help to find sites where such an optical system could perform at its greatest potential.

Oceanit has been simultaneously developing and building a near infrared camera system, during the HANDS-IONS program, to track geosynchronous satellites during the day. This effort along with the site modeling is predicted to create an effective system for daylight satellite tracking. The camera system contains a HgCdTe focal plane, refractive re-imaging optics, telescope-specific Lyot stops, and a filter wheel with *J*, *H*, *K-short*, and *K* filters [2,3]. The initial test of this camera system recently took place on Mauna Kea where the camera was mounted on the University of Hawaii 2.2-m telescope. The camera was designed with the versatility to mount at the Cassegrain focus of four telescopes including the Mt. Lemmon Observing Facility (MLOF) telescope in Arizona, the Willard L. Eccles Observatory in Utah, and the AMOS 1.6 meter on Haleakala.

To help predict the performance of the camera at the Haleakala site and to guide observing strategies, we model the daytime sky during the summer solstice when the Sun is at the northern most latitude and during the vernal equinox when it is above the equator. The sky brightness is modeled along the GEO belt and the brightness here changes with the changing position of the Sun.

Our previous work showed that using empirical weather and radiosonde data as a user-specified model for the summer solstice at Haleakala produces more accurate results than using the Mid-Latitude Winter model included with MODTRAN [1]. This finding remains to be confirmed since daytime sky brightness measurements are limited. So far we have compared our results to those of J. Rayner who took informal measurements on Mauna Kea at the NASA Infrared Telescope Facility (IRTF). His results show that at 45 degrees from the Sun the sky brightness ranges from 6 to 6.5 magnitudes in the *J*, *H*, and *K* filters [4]. Soon we will have sky brightness measurements taken with the HANDS-IONS camera and will be able to compare these to our models. Currently we are modeling how the sky brightness changes throughout the year and we begin by comparing a user-specified model of vernal equinox to that of the summer solstice.

2. MODTRAN

The MODerate resolution atmospheric TRANsmission code (MODTRAN) was used to model the radiance and transmittance of the daytime sky. “MODTRAN is a "narrow band model" atmospheric radiative transfer code. The atmosphere is modeled as stratified (horizontally homogeneous), and its constituent profiles, both molecular and particulate, may be defined either using built-in models or by user-specified vertical profiles” [5].

The atmosphere is modeled as thirty layers, each having different physical characteristics. Measured and modeled spectra of all of the dominant molecular and ionic components are included and multiple scattering from particles can be modeled. Wavelengths ranging from ultraviolet into the thermal infrared wavelengths can be modeled and the atmosphere is modeled out to 100 kilometers when using a built-in model.

MODTRAN can calculate lunar and solar positions at specified times and apply them to a model. Since we are interested in how the sky brightness changes through the day, we model 15 look angles along the GEO belt for each of 16 hours starting before sunrise and ending after sunset. This equates to 240 simulations for one day, as many input files, and a generous amount of processing time. To simplify input file preparation and lessen processing time, we wrote software to generate input files from a few base input files, and wrote a Perl script to distribute the simulations on a computer cluster. This method reduces the processing time from approximately 250 hours on a 3 GHz workstation to 2 hours on our 96-core, 2.4 GHz cluster.

The MODTRAN input file consists of many options for built-in models and user-specified models. Most notably the user-specified model was chosen in order to include weather and radiosonde data. In addition, solar azimuthal dependence, the spectrally dependent scattering mode, and the multiple-scattering model were selected. And, settings for aerosol models, visibility, and extinction were declared. MODTRAN inputs consist of many interdependent parameters and we have continued with a similar setup as in our previous models [1]. We used MODTRAN 5 for the results here; previously, we had used MODTRAN 4.

3. SIMULATION AND INPUT

3.1. MODTRAN

Using MODTRAN we simulated two user-specified models, one on the summer solstice day of year (DOY) 172 to 173 of 2010 and the other close to the vernal equinox on DOY 82 to 83 of 2007. The actual vernal equinox was on DOY 80 but because the weather measurements were not ideal on this date, we used the closest day with the best weather. To create a user-specified model in MODTRAN, we used two main categories of input values that need to be defined. One includes values of geometry such as site latitude and longitude, site altitude, and the azimuth and elevation of the angle of the atmosphere to be modeled. This is the same as the look angle to the center of the GEO belt as seen from our site. The other includes empirical weather and atmospheric data measured by radiosonde observations. These values are all tied together by the time of day.

3.2. GEO BELT POSITION

We model positions only along the GEO belt in order to constrain the many possible angles and to focus on this important part of the sky. Our primary purpose in performing these simulations is to find the best time to observe satellites here during the day. The position of the GEO belt as seen from Haleakala was found by using the geosynchronous catalog of element sets downloaded from www.space-track.org. To further constrain the position of the GEO belt, only satellites with an inclination of zero were kept. The remaining element sets were input to a program called SatView, which can output the elevation and azimuth of each satellite as a function of time. Any satellite with an elevation lower than 20 degrees was eliminated since the airmass becomes large below that elevation. Using the remaining list of satellites at this site reveals a lack of satellite positions near the highest elevations of the GEO belt. In order to represent these positions, a sixth order polynomial was fit to the existing positions. We then solved for positions along the GEO belt in 10-degree azimuthal steps. Each of 15 positions or “look angles” is modeled for each of 16 hours throughout the day. The resulting positions can be seen in Fig. 1.

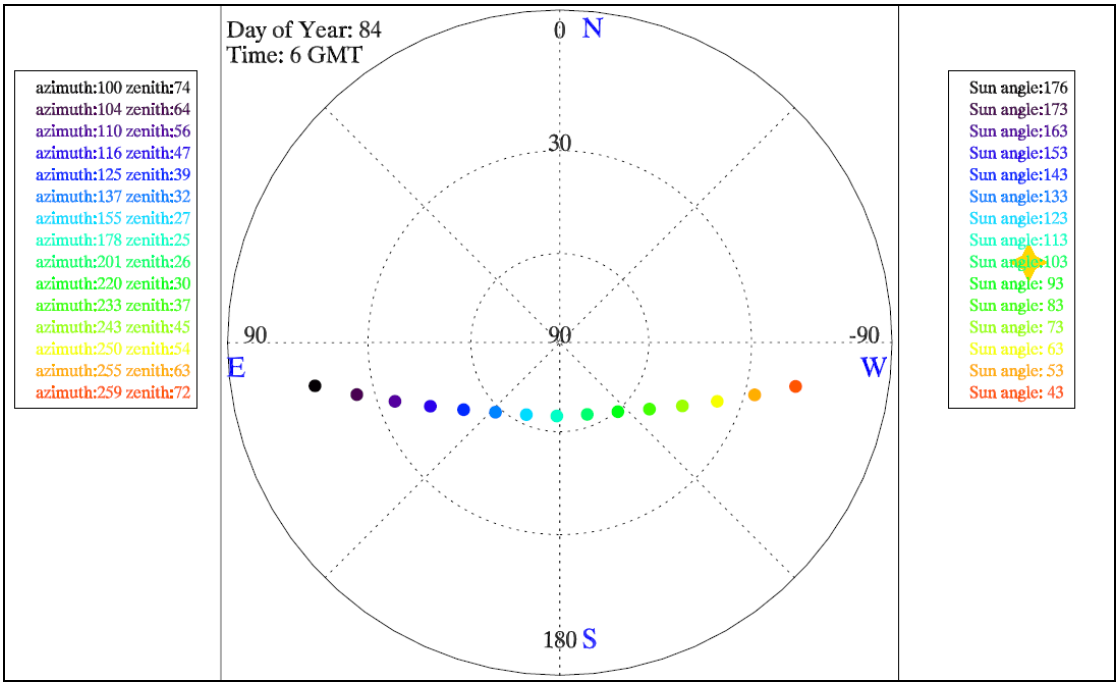

Fig. 1. This plot of the GEO belt positions also shows the position of the Sun at one of 16 times included in the model. The look angles are color-coded using the standard "rainbow" encoding, and these colors are used in subsequent plots. The lowest points toward the East and West are at 16° elevation, which are not likely to be used for real observations.

3.3. RADIOSONDE

The radiosonde observations measure wind direction, wind speed, temperature, pressure, dewpoint depression, and geopotential height. Most of these values can be used in their current format except for geopotential height, which is converted to altitude, and dewpoint depression, which is converted to dewpoint temperature in order to be input to MODTRAN. The radiosonde balloon is released at 00:00 UTC and 12:00 UTC each day. There are 1500 stations worldwide and we use data from the one in Hilo, Hawaii, which is located at the airport (ITO airport code). This data is available from the Integrated Global Radiosonde Archive (IGRA) website [6]. The radiosonde data we used had a maximum altitude of about 31 km, which is a potential source of error in our simulation.

3.4. WEATHER

The Mees Solar Observatory weather station records historical weather data, which we were able to use for both the summer equinox and the vernal equinox models [7]. Temperature, visibility, rain rate, current wind speed, and the 24-hour average wind speed are recorded for the past 18 years. This weather station provides all data needed for a user-specified model. We examined this data and historical visible and infrared satellite imagery of Hawaii from the GOES satellites to select the best days in recent years; these simulations represent a best-case scenario. While searching for data for other sites we have found that not all sites have stations with records as comprehensive as these, both in what is recorded and in temporal completeness. There are a few more parameter values to input that can easily be found or declared. Since the temperature satisfies the lower boundary temperature parameter in MODTRAN, which depends on the altitude of the site, we also input this value. Similarly, all measured values are associated with the input parameter values time of day and day of year. The values in the data set shown in

Table 1 each have an associated MODTRAN parameter [8].

Table 1. A representative set from 16 hourly weather data sets for Haleakala day of year 83.

Day of Year	83
Decimal Time	17.00 UTC
Wind	8.46 m/s
Temperature	281.61 °K
Visibility	50.000 km
Ground Altitude	3 km
Rain Rate	0 mm/hr
24-hr ave. Wind Speed	7.00 m/s

4. RESULTS AND DISCUSSION

The sky radiance and transmittance of both the summer solstice and vernal equinox is shown in Fig. 2 and Fig. 3. Both are shown as a function of wavelength and look angle. In the transmittance plots the positions of the *J*, *H*, and *K* filters can be seen. Their central wavelengths are 1.24, 1.65, and 2.20 μm respectively [9]. Plots showing the performance of the *J* and *K* filters within the comparison of the two modeled dates are shown in Fig. 6 and Fig. 7.

Near 3 μm, note that there is a lack of some known features in the radiance that were shown in our previous work where we showed a comparison of the built-in model to the user-specified model [1]. The built-in model only shows these features near 3 μm. Since the radiosonde observations reach a maximum altitude of 31 km while the built-in model reaches 100 km, we suspect that this difference is the reason for not seeing those features in the user-specified model. It is clear that for future modeling, we need to include the atmospheric layers above 31 km. We plan on doing this by merging the Mid-Latitude Winter model with the radiosonde model to fill the gap at higher altitudes.

The plots for both dates are not shown with matching times of day because the Sun is at a different elevation at each hour modeled. To compare the most similar cases 06:00 AM local time is shown for the summer solstice and 07:00 AM local time for the vernal equinox. At these two times the Sun is at the most similar elevation and the main difference is the azimuth of the Sun.

The radiance is greater on the vernal equinox and the Sun is also much closer to the GEO belt. On both radiance plots the back scattering can be seen as the look angles farthest from the Sun are brighter than those closer to the Sun near zenith. The effects of polarization are not included in this version of MODTRAN, but version 5.2-p, was recently released, and it does include polarization effects. We plan on trying this version for our future simulations.

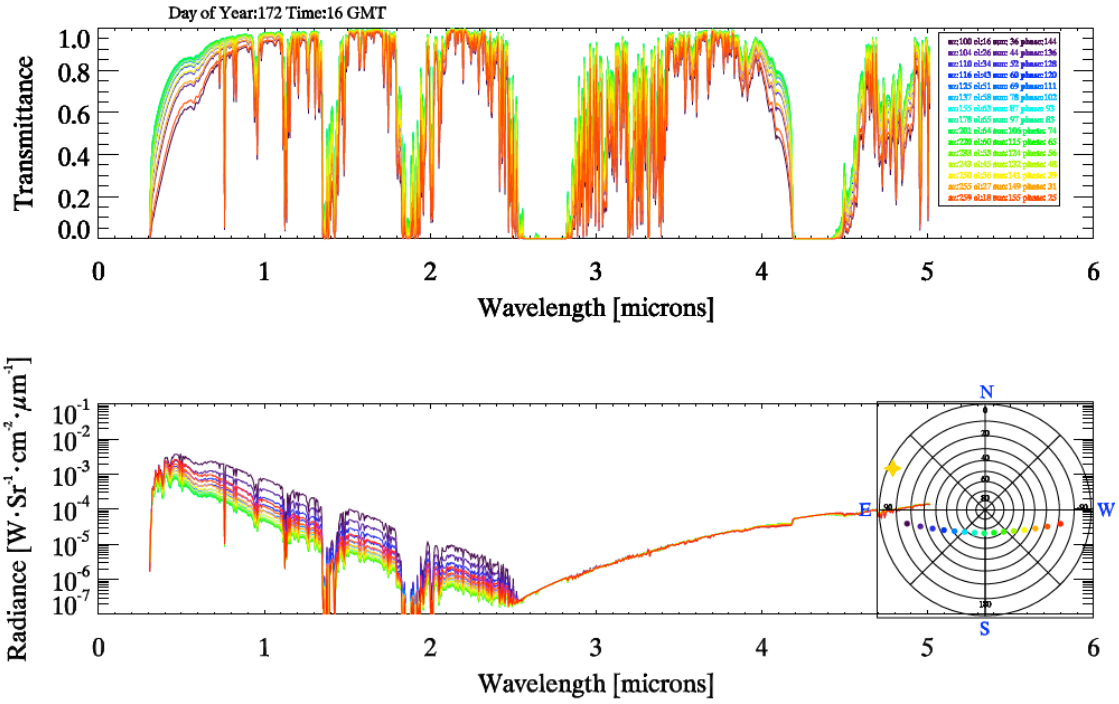

Fig. 2. The transmittance and sky radiance for Haleakala on the summer solstice at 0600 local time. Note the position of the Sun shown by the yellow star in the polar plot. Each color represents the look angles shown in the polar plot. The lack of variation above 3 μm is not real (see text).

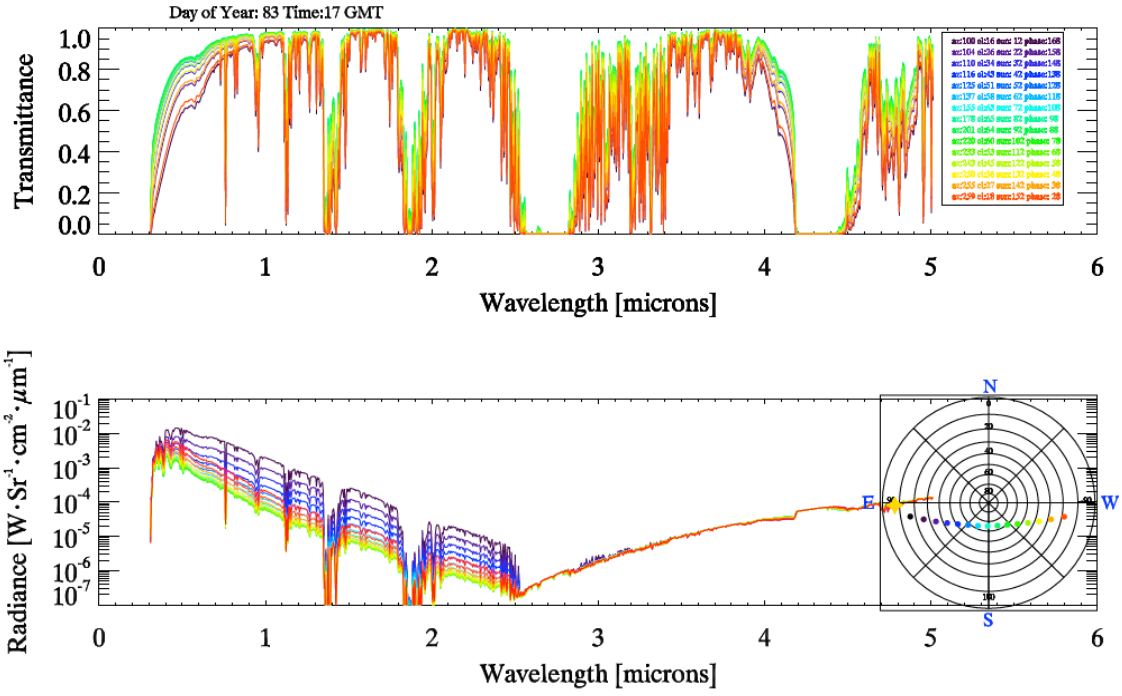

Fig. 3. The transmittance and sky radiance for Haleakala on the vernal equinox at 0700 local time. The radiance is greater than during summer solstice and the Sun is at approximately the same elevation as in the winter solstice but closer to the GEO belt.

The changes in radiance throughout the day are more significant than the changes in transmittance. Radiances through the first half of the day for summer solstice are shown in Fig. 4 while for vernal equinox they are shown in Fig. 5. When the Sun is at lower elevations the differences between the radiances of the look angles is greatest, while when the Sun is at its highest elevation the radiances are the most similar.

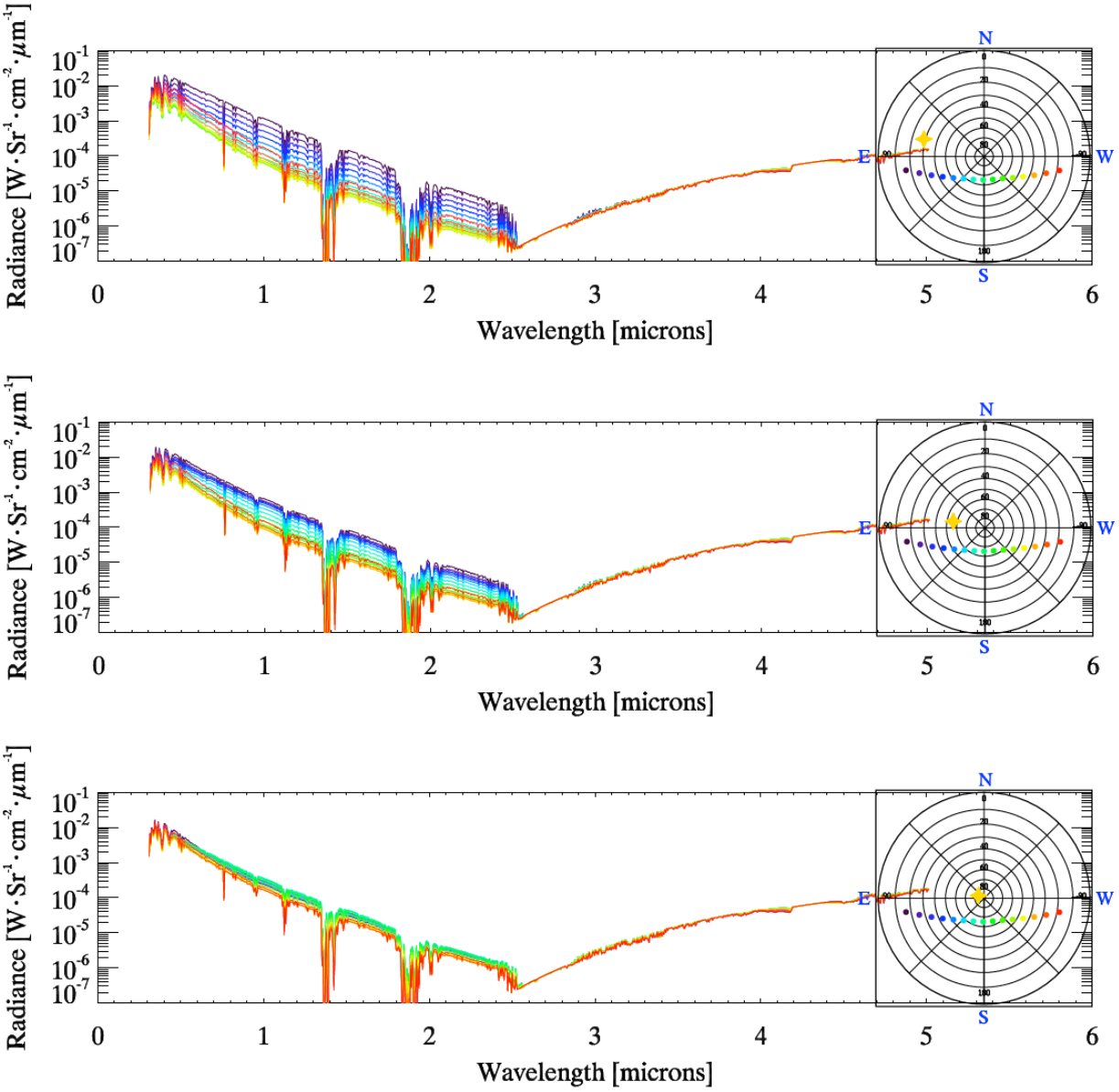

Fig. 4. Sky radiances for all look angles become the most similar when the sun is near its highest elevation. Here they are shown on the morning of the summer solstice at 8AM, 10AM, and 12PM local time, from top to bottom. The Sun's position can be seen on the polar plot.

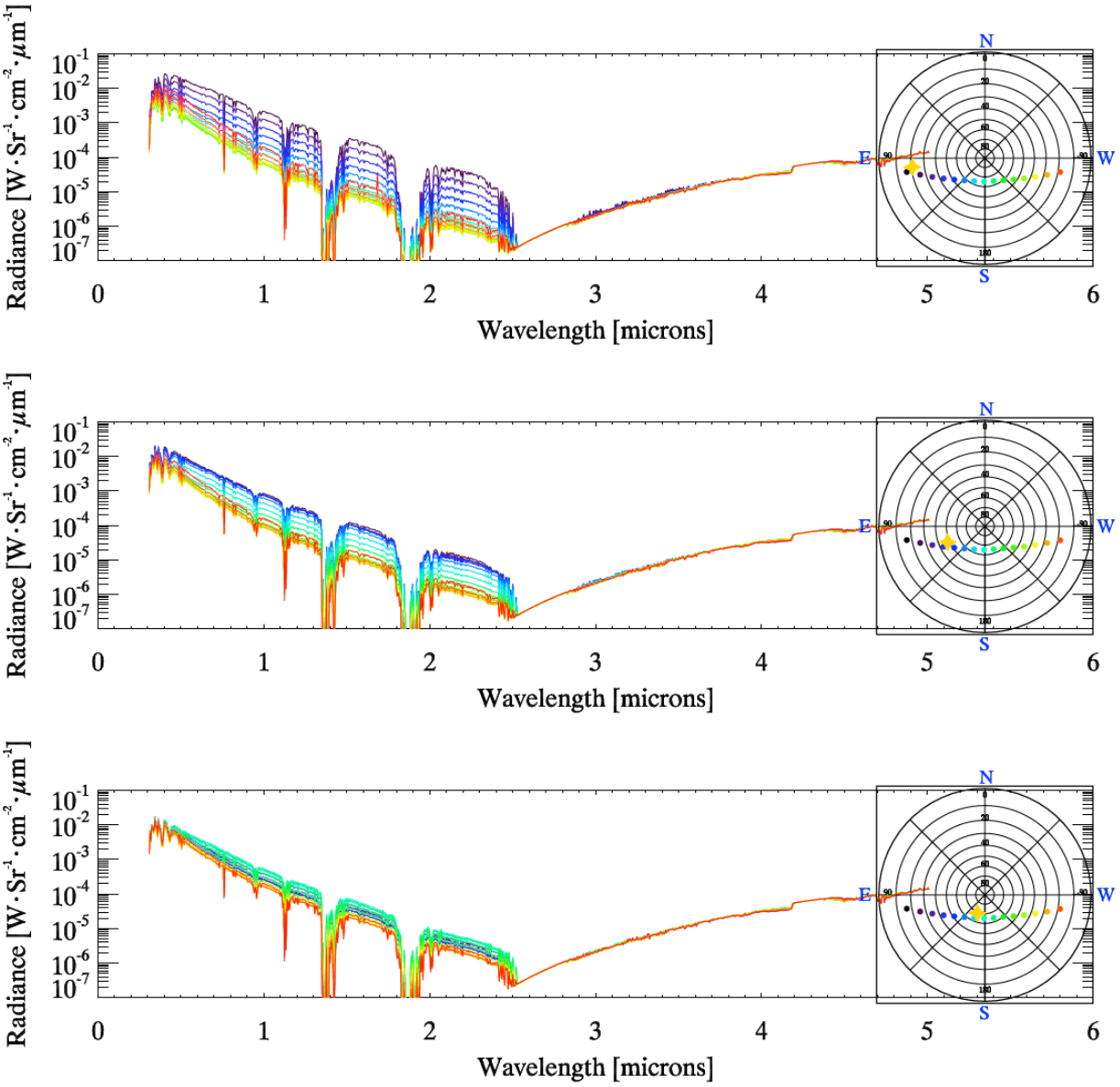

Fig. 5. Like in the summer solstice plots, sky radiances for all look angles become the most similar when the sun is near its highest elevation. Here they are shown on the morning of the vernal equinox at 8AM, 10AM, and 12PM local time. The Sun's positions in Fig. 4 were farther from the GEO belt and here they are following it closely. Note that the Sun's elevations are not the same on both dates because the times are the same. If time is only considered, the variation in sky radiance between look angles is greater at 8AM on the vernal equinox than on summer solstice.

The magnitude of the sky in *J* and *K* filters is plotted as a function of local time, in Fig. 6, for each look angle and for both dates. The magnitude is calibrated using Vega as a reference of 0^{th} magnitude. On the vernal equinox there is a greater variation in sky magnitude between look angles and for both dates the sky is dimmer in the *K* band. The lowest look angles become brighter by at least half a magnitude on the vernal equinox than on the summer solstice but none are significantly dimmer. Again, evidence of backscattering can be seen at a time near sunrise when the look angles farthest from the sun (red) are brighter than those at the highest elevations. This can also be seen near sunset. The sky brightness has the greatest variation at look angles closer to the horizon and the least variation at look angles at the highest elevations. Note that the sky is generally slightly brighter in the beginning of the day than at the end. All in all, the summer solstice is a better time of year to observe the GEO belt from Haleakala than the vernal equinox.

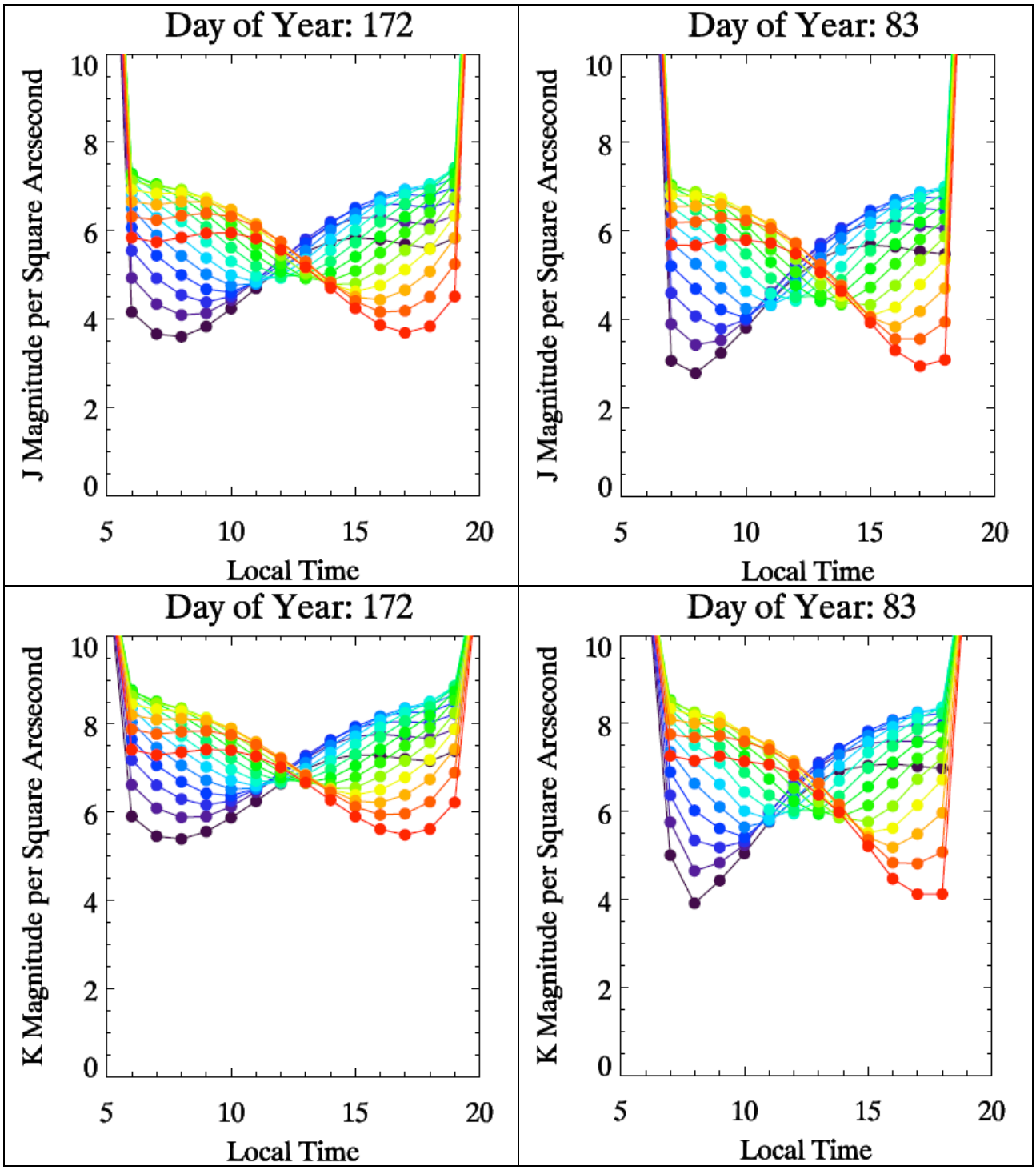

Fig. 6. The magnitude of the sky at each look angle changes with time. Each color represents a look angle as shown in previous plots. The redder colors are closer to west while the darkest purple colors are the closest to east. The sky becomes brighter at all look angles on the vernal equinox than on the summer solstice because the Sun's angular distance is much closer to the look angles on this day. The lowest look angles show that the magnitude can be 1 magnitude dimmer on the summer solstice.

The magnitude of the sky as it changes with the angle to the Sun is shown in Fig. 7. The sky appears to be brighter on the vernal equinox though the angle to the Sun is the same for both dates. It is not apparent why this effect is seen and it may require additional simulations to find the cause.

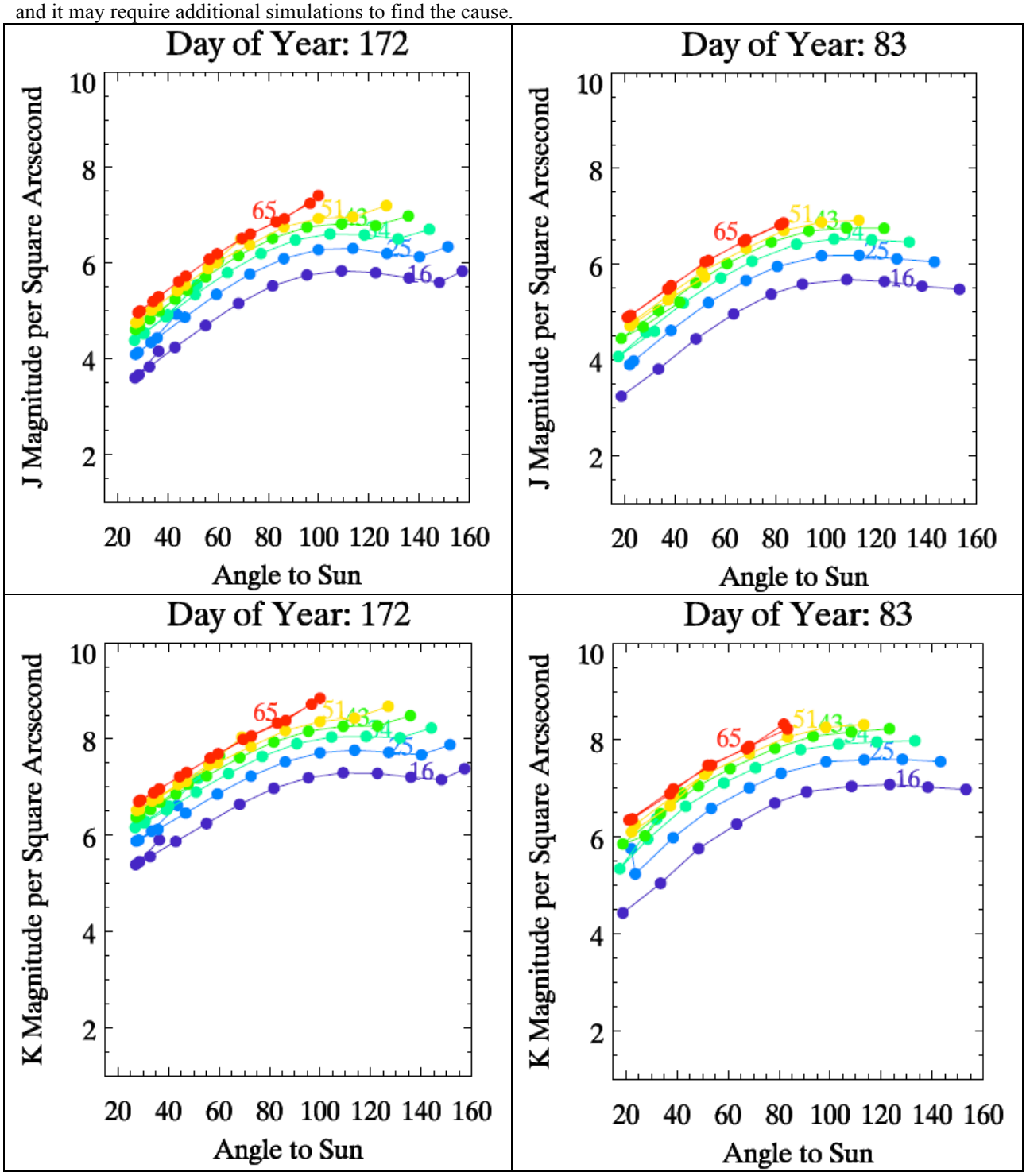

Fig. 7. The sky brightness, in magnitudes per square arcsecond, for *J* and *K* filters on both dates changes with the angle to the Sun. The colored numbers on each line represent the altitude, in degrees, of a look angle on the GEO belt. In general, as the Sun gets closer to a look angle the sky gets brighter. Lower look angles are brighter than higher look angles through a range of Sun separation angles. Between the two days, no look angle gets significantly dimmer but the lowest look angles do become brighter on the vernal equinox.

5. CONCLUSION AND FUTURE WORK

Sky radiance and transmittance at Haleakala was modeled from 0.3 to 5 μm using MODTRAN and its capability to accept weather and radiosonde data to create a user-specified model. This was done for 15 positions along the GEO belt on two dates, one on the summer solstice and one near the vernal equinox to characterize the difference of the sky brightness when the Sun is closer and farther from the GEO belt. For both dates the comparison of *J* and *K* sky magnitudes shows that the sky is dimmer in the *K* band.

On the vernal equinox the Sun follows the GEO belt more closely than on the summer solstice. This results in a greater variation of sky brightness between the look angles. The dimmest brightness on both dates is similar for all times of day, but the sky at each look angle is brighter on the vernal equinox. The summer solstice, surprisingly, is a better time to observe the GEO belt during the day, since the sky can be 1 magnitude per square arcsecond dimmer than at the vernal equinox.

To understand this better, the plot of sky magnitude as a function of the angle to the Sun in Fig. 7 was created. It shows that the closer the Sun is to a particular elevation in the GEO belt, the brighter the sky is at this location. Interestingly, the lowest look angle at 16 degrees elevation most notably shows that the sky is brighter through the sun angles on the vernal equinox. It is not understood why, though the angle to the sun is the same in both cases, the sky magnitude is brighter on the vernal equinox. Additional simulations could help to make the reason apparent.

In the future we would like to model the winter solstice to understand more fully the effect of the Sun's position on sky brightness throughout the year. Adding even more models through the year would give us the opportunity to characterize the sky brightness as it changes with the day of year. This would require an average of weather data around each date in order to eliminate the effects of any exceptional weather data. In addition, we will merge the upper atmospheric standard models with the radiosonde models for greater accuracy in the radiance plots and integrated sky magnitudes above 2.5 μm in wavelength. We use these models of radiance and transmittance to predict the signal to noise ratios (SNR) of GEO satellites to guide our observation strategies. Since we recently collected some images of the daytime sky with the HANDS-IONS camera we will have some real measurements to compare to our models.

This work is sponsored by the Advanced Technology Branch of the Space and Missile Systems Center (AFSPC SMC/SYE) under contract FA8819-10-C-002, High Accuracy Network Determination System – Intelligent Optical Networks for Space Situational Awareness (HANDS-IONS), with program manager Capt. David Schill. The authors gratefully acknowledge the insight and advice of Dr. Donald Davies and Dr. Ray Russell of the Aerospace Corporation.

6. REFERENCES

1. Jim, K., Gibson, B., Pier, Ed., *Daytime Sky Brightness Modeling of Haleakala*, Proceedings of the Advanced Maui Optical and Space Surveillance Technologies Conference, held in Wailea, Maui, Hawaii, September 2011.
2. Jim, K.,Wolfshagen, R., Gibson, B., Pier, Ed., Hodapp, K., Onaka, P., *The HANDS-IONS Daytime Camera for GEO Satellite Characterization*, Proceedings of the Advanced Maui Optical and Space Surveillance Technologies Conference, held in Wailea, Maui, Hawaii, September 2011.
3. Jim, K., Wolfshagen, R., Gibson, B., Kokubun, D., Cognion, R., Hodapp, K., Onaka, P., *Daytime GEO Satellite Characterization with the HANDS-IONS Camera*, Proceedings of the American Institute of Aeronautics and Astronautics (AIAA) SPACE 2012 Conference, held in Pasadena, California, September 2012, in preparation.
4. Rayner, J., NASA IRTF, Institute for Astronomy, University of Hawaii, private communication, 2010.
5. MODTRAN5, 2012, http://modtran5.com/about/index.html.
6. Integrated Global Radiosonde Archive, 2012, http://www.ncdc.noaa.gov/oa/climate/igra/.
7. Kuhn, J., Institute for Astronomy, University of Hawaii, private communication, 2010.
8. Berk, A., Anderson, G.P., Acharya, P.K., Shettle, E.P., *MODTRAN 5.2.0.0 User's Manual*, Spectral Sciences, Inc., Burlington, MA and AFRL, Space Vehicles Directorate, Hanscom AFB, MA, 2008.
9. Simons, D.A., Tokunaga, A., *The Mauna Kea Observatories Near-Infrared Filter Set. I. Defining Optimal 1–5 Micron Bandpasses*, Publications of the Astronomical Society of the Pacific, Vol. 114, No. 792 (February 2002), pp. 169-179.